Applied Catalysis A: General 400 (2011) 91–98

Contents lists available at ScienceDirect

Applied Catalysis A: General

journal homepage: www.elsevier.com/locate/apcata

Trifluoromethanesulfonic acid immobilized on zirconium oxide obtained by the sol–gel method as catalyst in paraben synthesis

Marina Gorsd, Luis Pizzio, Mirta Blanco*

Centro de Investigación y Desarrollo en Ciencias Aplicadas “Dr. J.J. Ronco” (CINDECA), Departamento de Química, Facultad de Ciencias Exactas, UNLP-CCT La Plata, CONICET, 47 No 257, 1900 La Plata, Argentina

ARTICLE INFO

Article history:
Received 30 November 2010
Received in revised form 11 April 2011
Accepted 16 April 2011
Available online 22 April 2011

Keywords:
Trifluoromethanesulfonic acid
Zirconium oxide
Sol–gel
Catalyst
Parabens

ABSTRACT

The parabens, alkylic esters of p-hydroxybenzoic acid, were synthesized using trifluoromethanesulfonic acid immobilized on zirconium oxide (zirconia) as catalyst. The oxide was obtained by the sol–gel method, using urea as a pore-forming agent. After removing urea by extraction with water, the solid was dried and then calcined at 100, 205, 310 and 425 °C for 24 h. Afterward, it was impregnated with trifluoromethanesulfonic acid in toluene at reflux and leached to remove the weakly adsorbed acid. Mesoporous materials were obtained, whose mean pore diameter increased with the temperature of the thermal treatment of the support, while the specific surface area and the amount of acid bonded to the support decreased. The samples are crystalline from 400 °C and are thermally stable up to 250 °C. The catalysts have strong acidity and the number of acid sites decreased with the acid content in the support. The catalytic activity in the synthesis of propyl paraben, expressed as moles of ester formed at 5 h/mol acid in the catalyst, decreased when samples obtained from supports thermally treated at higher temperature were used. The activity also slightly diminished for the synthesis of different parabens in the order propyl > ethyl > methyl ester.

© 2011 Elsevier B.V. All rights reserved.

1. Introduction

The parabens are esters of p-hydroxybenzoic acid, which are widely used as preservatives in food and also in cosmetics. They are antimicrobial agents, being more active against fungi and yeast rather than against bacteria.

The esters of p-hydroxybenzoic acid were obtained with the purpose of replacing salicylic and benzoic acids, both of which have the drawback of being effective only in the highly acid pH range, assuming that the esters might be advantageous in this aspect since they have a wide pH range [1]. Recently, excellent reviews have been published about parabens, which deal not only with their properties and uses, but also report toxicological and risk assessment studies [2–4].

The antimicrobial action of p-hydroxybenzoic acid esters increases with the chain length, but the solubility decreases; hence, in practice, the esters with shorter chain length are commonly used.

The parabens are obtained through the reaction of the corresponding alcohol with p-hydroxybenzoic acid, usually catalyzed by acids. Due to the increasing awareness about environmental care, it is advisable to use solid catalysts to avoid the use of mineral acids, which generate a large amount of acid waste. At the same time, they allow for easy product and catalyst separation, thus decreasing the need of the classical separations by distillation or extraction.

The heterogeneization of trifluoromethanesulfonic acid (CF_3SO_3H) by immobilization on a suitable support is an interesting alternative to contribute to the field of clean processes. This acid, also named triflic acid, has a highly acidic nature and an excellent thermal stability; it also has good resistance to reductive and oxidative dissociation, with no generation of fluoride ions [5].

The trifluoromethanesulfonic acid was used as an efficient homogeneous catalyst in many organic reactions, such as polymerization and acylation [6,7], among others, but has environmental disadvantages because the recovery of triflic acid (Tri) from the reaction mixture results in the formation of large amounts of waste.

Papers dealing with Tri heterogeneization are scarce, though its immobilization on zirconium hydroxide for its use in the biphenyl benzoylation reaction [8], and in the synthesis of flavones and chromones immobilized on carbon [9] or titania [10] has been reported.

With the purpose of making a contribution to a little explored field and as a continuation of previous work, the preparation and characterization of new catalysts obtained by impregnation of trifluoromethanesulfonic acid on zirconia prepared by the sol–gel method, using zirconium propoxide as precursor, and urea as a nonsurfactant low-cost pore-forming agent, is reported.

---

* Corresponding author. Tel.: +54 221 421 1353; fax: +54 221 421 1353.
E-mail address: mnblanco@quimica.unlp.edu.ar (M. Blanco).

0926-860X/$ – see front matter © 2011 Elsevier B.V. All rights reserved.
doi:10.1016/j.apcata.2011.04.018

The effect of the calcination temperature of the support on the physicochemical, acidic and textural characteristics of the catalysts was studied. The catalytic behavior of the prepared materials in paraben synthesis was firstly studied through the esterification of p-hydroxybenzoic acid with propyl alcohol in a conventional batch glass reactor at atmospheric pressure. In addition, the efficiency of the obtained catalysts was tested in the esterification of p-hydroxybenzoic acid with methanol, ethanol and n-propanol in an autoclave reactor at the self-generated pressure. The results are correlated with the catalyst properties.

2. Experimental

2.1. Support preparation

Zirconium propoxide (Aldrich, 26.6 g) was mixed with absolute ethanol (Merck, 336.1 g) and stirred for 10 min to obtain a homogeneous solution under N_2 at room temperature. Then 0.47 cm^3 of 0.28 M HCl aqueous solution was dropped slowly into the above mixture to catalyze the sol–gel reaction.

After 3 h, an appropriate amount of urea–alcohol–water (1:5:1 weight ratio) solution was added to the hydrolyzed solution under vigorous stirring to act as template. The amount of added solution was fixed in order to obtain a template concentration of 10% by weight in the final material.

The gel was kept in a beaker at room temperature up to dryness. The solid was ground into powder and extracted with distilled water for three periods of 24 h, in a system with continuous stirring, to remove urea. Afterwards, portions of the obtained solid were calcined at 100, 205, 310, or 425 °C for 24 h, thus obtaining the supports identified as Zr_{T100}, Zr_{T200}, Zr_{T300}, and Zr_{T400}, respectively.

2.2. Catalyst preparation

Trifluoromethanesulfonic acid (0.01 mol, Alfa Aesar) was added dropwise to a mixture of Zr_{TX} (2 g) and toluene (20 cm^3, Merck) at 90 °C under nitrogen atmosphere; then it was further refluxed for 2 h. Next, the sample was cooled, filtered, washed with acetone (Mallinckrot AR) and dried at 100 °C for 24 h.

The solids were then extracted with a mixture of dichloromethane and diethyl ether (40 cm^3/g of solid) for three periods of 4 h in order to remove the acid weakly attached to the support. Afterwards, they were dried again at 100 °C for 24 h. The amount of trifluoromethanesulfonic acid retained in the solids was determined by C and S elemental analysis with a Carlo Erba EA1108. The samples were named $TriZr_{T100}$, $TriZr_{T200}$, $TriZr_{T300}$, and $TriZr_{T400}$.

2.3. Solid characterization

The characterization of the thermal properties of the supports and the catalysts was performed by thermogravimetric (TGA) and differential scanning calorimetric (DSC) analyses, with a Shimadzu DT 50 thermal analyzer. The measurements were carried out under argon, with a 25–50 mg sample, and a heating rate of 10 °C/min, using quartz cells as sample holders and α-Al_2O_3 as reference.

The textural properties of the solids were determined from N_2 adsorption–desorption isotherms at the liquid-nitrogen temperature. They were obtained using Micromeritics ASAP 2020 equipment. The samples were previously degassed at 100 °C for 2 h.

X-ray diffraction (XRD) patterns of the solids were recorded with Philips PW-1732 equipment, using Cu Kα radiation, Ni filter, 20 mA and 40 kV in the high voltage source, a 5–60° 2θ scanning angle range, and a scanning rate of 1° per min.

Table 1
Trifluoromethanesulfonic acid amount in the catalysts.

Sample	N_{Tri} (mmol CF_3SO_3H/g)	W_{Tri} (mmol CF_3SO_3H/g)
$TriZr_{T100}$	0.91	0.88
$TriZr_{T200}$	0.53	0.49
$TriZr_{T300}$	0.41	0.38
$TriZr_{T400}$	0.10	0.11

Fourier transform infrared (FT-IR) spectra of the samples were recorded using Bruker IFS 66 FT-IR equipment, pellets with approx. 1% w/w of the sample in KBr, in a measuring range of 400–4000 cm^{-1}.

The acidity of the solids was measured by means of potentiometric titration. A known mass of solid was suspended in acetonitrile and stirred for 3 h. Then, the suspension was titrated with 0.05 N n-butylamine in acetonitrile solution at a flow of 0.05 cm^3/min, measuring the electrode potential variation in a digital pH meter Hanna 211 with a double-junction electrode.

2.4. Paraben synthesis

The esterification of p-hydroxybenzoic acid with propyl alcohol to obtain propyl paraben was carried out in liquid phase at 100 °C in a 50 ml batch glass reactor equipped with a condenser and a magnetic stirrer. The reagent mixture was heated under stirring and then the catalyst was added. An n-propanol:p-hydroxybenzoic acid:catalyst molar ratio of 10:1:0.1 was used. Samples were periodically taken and analyzed by gas chromatography in a Shimadzu GC-14B chromatograph with TC detector, and using dodecane as internal standard.

The esterification was also performed in a 15 ml autoclave reactor heated up to 100 °C, at the self-generated pressure, using the same reagent molar ratio mentioned above, not only to evaluate the catalyst performance in this type of reactor for the esterification of p-hydroxybenzoic acid with n-propanol, but also with ethanol and methanol, in order to obtain propyl, ethyl and methyl parabens. After 5 h under reaction, the analysis of the reaction mixture was performed by gas chromatography.

3. Results and discussion

The amount of trifluoromethanesulfonic acid attached to the support (N_{Tri}), calculated from the elemental analysis, decreased with the increment of the thermal treatment temperature of the support (Table 1). This effect may be explained if the interaction between the trifluoromethanesulfonic acid and zirconia is assumed to be of electrostatic type due to proton transfer to the –OH groups on the support surface with subsequent water evolution

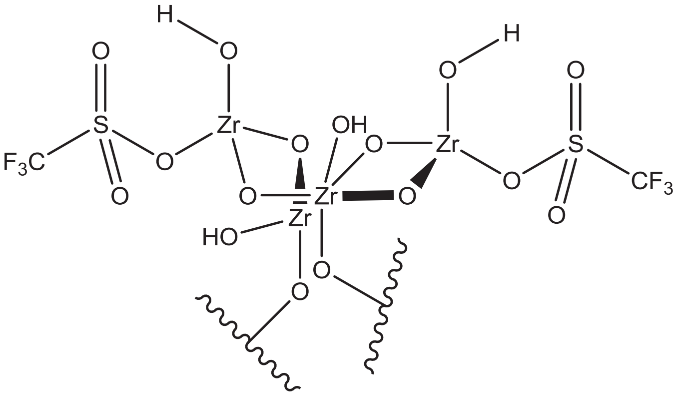

Scheme 1.

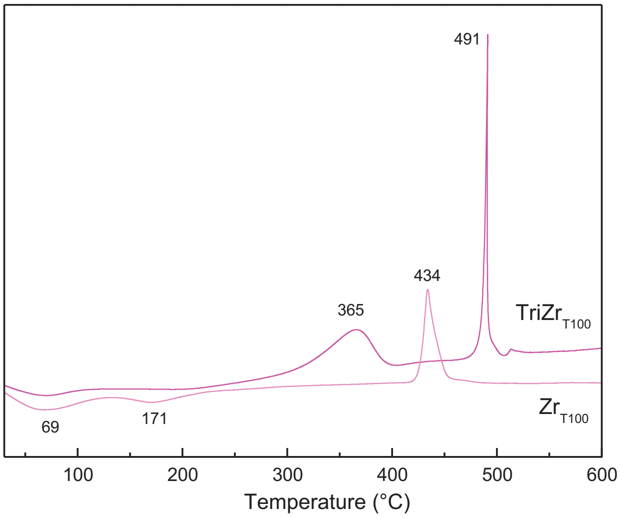

Fig. 1. DSC diagrams of the Zr$_{T100}$ and TriZr$_{T100}$ samples.

(Scheme 1). So, as a result of the support dehydroxylation during the thermal treatment, the amount of OH groups to be protonated decreases, and therefore N_{Tri} diminishes.

The DSC diagram of the Zr$_{T100}$ support (Fig. 1) showed two endothermic peaks at 69 and 171 °C, attributed to the loss of physically adsorbed water, and the partial dehydroxylation of the solid, respectively. There was also an exothermic peak at 434 °C, which was assigned to zirconia transformation from an amorphous to a crystalline phase.

In the DSC diagram of the TriZr$_{T100}$ catalyst (Fig. 1), the last peak appeared shifted to higher temperatures (491 °C), indicating that the trifluoromethanesulfonic acid retards zirconia crystallization. The samples obtained by impregnation of the supports calcined at 205, 310, and 425 °C showed similar characteristics. This exothermic peak appeared at 494 and 487 °C in the diagrams corresponding to the TriZr$_{T200}$ and TriZr$_{T300}$ samples, and it is absent in that of the TriZr$_{T400}$ sample up to 500 °C (Fig. 2). A similar shift of the exothermal peak maximum was previously reported for samples containing molybdenum oxide or copper oxide on zirconia [11], for zirconia doped with nickel or aluminum [12], and for zirconia with sulfate or chromate addition [13]. These authors agree in that the stability increase of the hydrated zirconium oxide is related to an inhibitory effect in zirconia crystallization induced by a good dispersion of this type of additive.

Additionally, in all the samples containing trifluoromethanesulfonic acid, another exothermal peak appeared in the range 350–370 °C, ascribed to acid elimination. The intensity of this peak diminished in parallel with the N_{Tri} decrease.

The TGA diagram of the Zr$_{T100}$ support (Fig. 3) showed that dehydration takes place in three main steps. The first step, below 120 °C, is due to the evolution of physically adsorbed water and the second, in the temperature range 120–250 °C, to the loss of structural water. Above 250 °C, a small weight loss takes place, which can be assigned to the decomposition of $Zr(OH)_4$ into ZrO_2.

The TGA patterns showed that the catalysts are thermally stable up to 250 °C, and from this temperature on, acid evolution begins.

From the comparison of the TriZr$_{T100}$ catalyst with the Zr$_{T100}$ support (Fig. 3), it is clearly observed that the evolution of the adsorbed acid takes place at temperatures between 250 °C and 400 °C, an effect that appeared in the DSC diagram as an exothermic peak with a maximum at 365 °C (Fig. 1). A similar behavior was observed in the TGA diagrams of the catalysts obtained from the supports calcined at 205, 310 and 425 °C (Fig. 4).

The amount of acid estimated from the TGA diagrams (W_{Tri}) is in close agreement with the amount of acid firmly attached to the support (N_{Tri}) calculated from the elemental analysis, (Table 1).

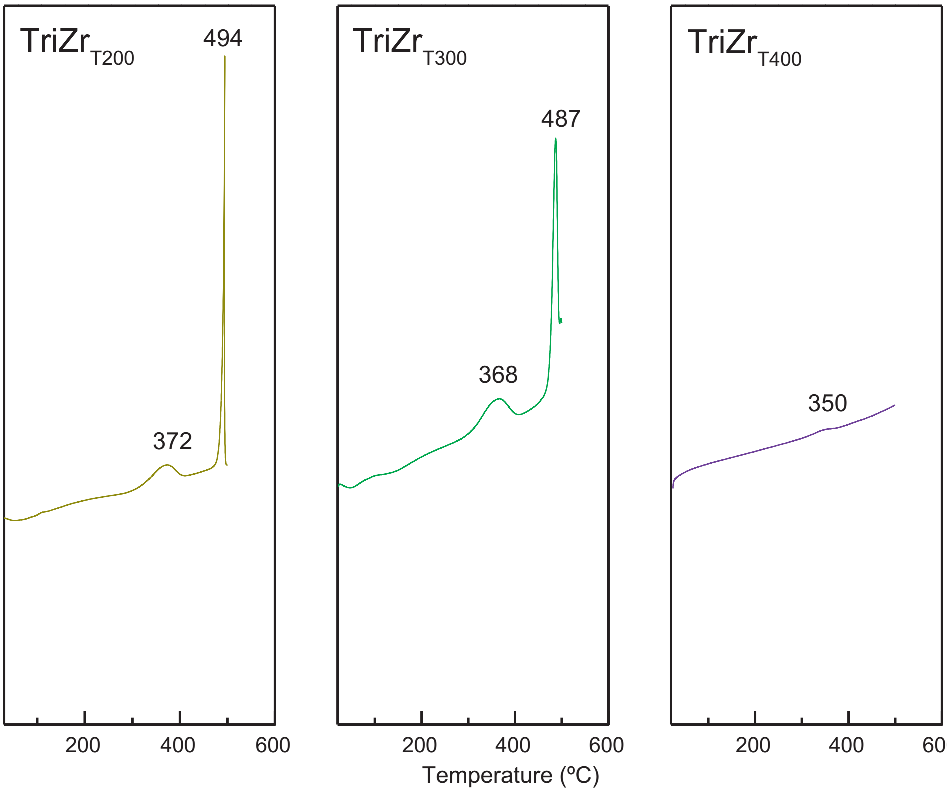

Fig. 2. DSC diagrams of the TriZr$_{T200}$, TriZr$_{T300}$ and TriZr$_{T400}$ catalysts.

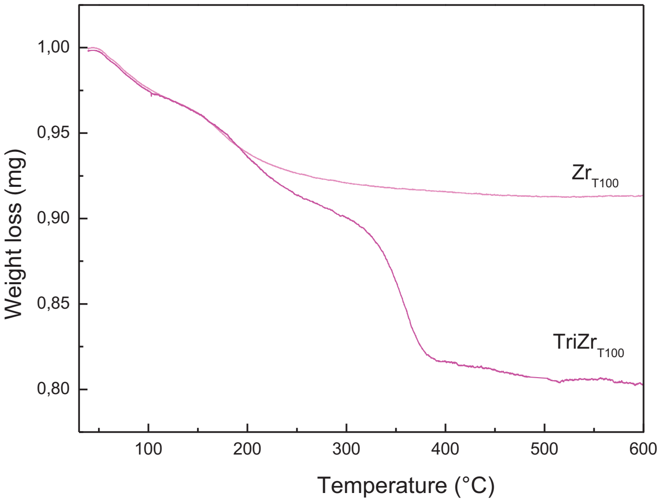

Fig. 3. TGA diagrams of the Zr_{T100} and $TriZr_{T100}$ samples.

W_{Tri} was calculated using the following expression:

$$W_{Tri} = (W_{TriZrTx} - W_{ZrTx})/FW_{Tri}$$

where $W_{TriZrTx}$ = weight loss of $TriZr_{Tx}$ catalyst from 250 °C to 600 °C (mg/g). W_{ZrTx} = weight loss of Zr_{Tx} support from 250 °C to 600 °C (mg/g). FW_{Tri} = CF_3SO_3H molecular weight.

The textural properties of the samples were determined from the N_2 adsorption–desorption isotherms at the liquid-nitrogen temperature. The isotherms obtained can be classified as type IV, characteristic of mesoporous materials, hysteresis being hardly visible, which is attributed to an ordered arrangement of the mesopores present in the material, as was reported for MCM-41 mesoporous materials [14].

Table 2
Textural properties of the supports calcined at different temperatures.

Sample	S_{BET} (m^2/g)	S_{Micro}[a] (m^2/g)	V_P (cm^3/g)	Micropore volume[a] (cm^3/g)	D_P[b] (nm)
Zr_{T100}	192	88	0.18	0.05	3.7
Zr_{T200}	132	50	0.16	0.02	4.7
Zr_{T300}	78	17	0.11	0.01	5.5
Zr_{T400}	20	0	0.07	0	14.2

[a] Micropore specific surface area and volume estimated by the *t*-plot method.
[b] Mean pore diameter obtained from the specific BET surface area.

The specific surface area (S_{BET}) of the supports, together with the average pore diameter (D_P) obtained from the Brunauer–Emmett–Teller pore size distribution, the total pore volume (V_P) estimated from the value corresponding to a ratio $p/p_0 = 0.98$, the micropore specific surface area (S_{Micro}) and the micropore volume, both estimated from the *t*-plot method, are gathered in Table 2.

The values of D_P were higher than 3.7 nm, so mainly mesoporous materials were obtained, with V_P being significantly higher than the micropore volume. While D_P increased with the temperature of the thermal treatment, both S_{BET} and S_{Micro}, and V_P decreased with the increment of the calcination temperature. At the same time, the micropore contribution to the total value of surface and volume also diminished. On the other hand, the textural properties of the catalysts were almost the same as those of the supports, thus indicating that they are not altered by trifluoromethanesulfonic acid addition, in a similar way to the report about the same acid supported on titanium dioxide [15].

The XRD patterns of the support calcined at 100, 205, and 310 °C (Fig. 5) showed a broad band at $2\theta = 30°$ attributed to their low

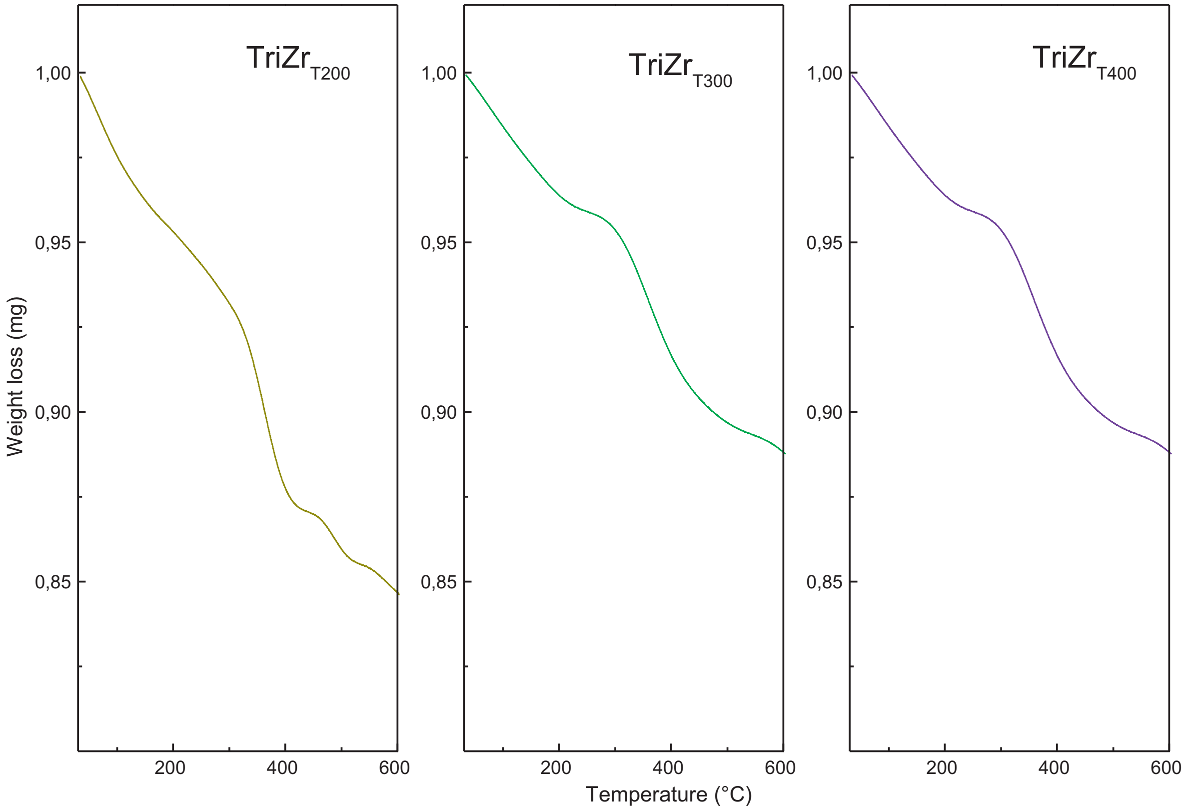

Fig. 4. TGA diagrams of the $TriZr_{T200}$, $TriZr_{T300}$ and $TriZr_{T400}$ catalysts.

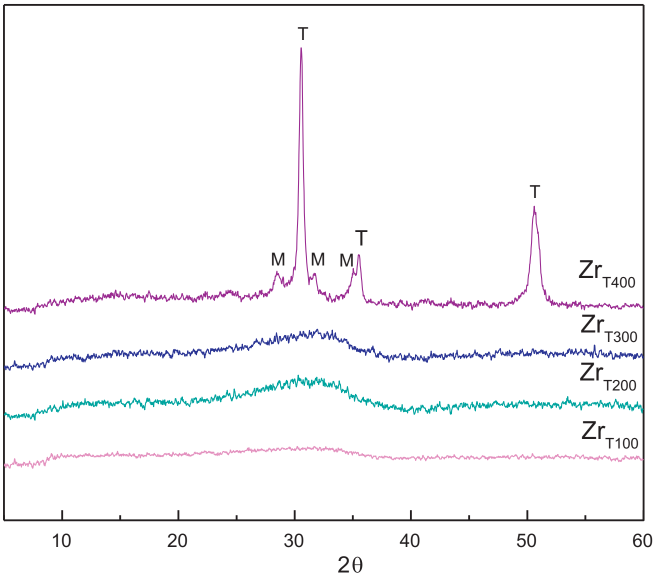

Fig. 5. XRD diagrams of the Zr$_{T100}$, Zr$_{T200}$, Zr$_{T300}$, and Zr$_{T400}$ supports. (T): peaks assigned to the tetragonal phase. (M): peaks assigned to the monoclinic phase.

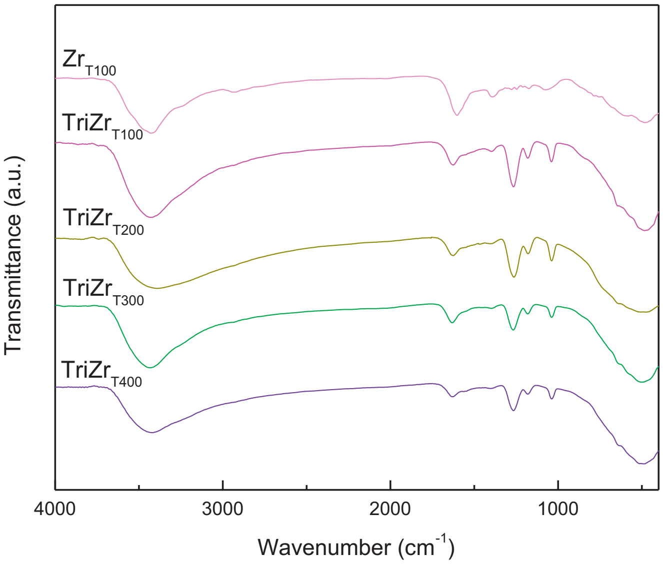

Fig. 6. FTIR spectra of the Zr$_{T100}$ support, and TriZr$_{T100}$, TriZr$_{T200}$, TriZr$_{T300}$, and TriZr$_{T400}$ samples.

crystallinity. In turn, the pattern of the Zr$_{T400}$ support showed peaks with maxima at $2\theta = 28.5$, 30.5, 31.7, 35.0, 35.5 and 50.6° assigned to the metastable tetragonal phase of zirconia, which is the main phase present though it is accompanied by a minor amount of the monoclinic phase of zirconia, as indicated in Fig. 5.

The XRD patterns of the catalysts (TriZr$_{T100}$, TriZr$_{T200}$, TriZr$_{T300}$, and TriZr$_{T400}$) showed features similar to those of the corresponding supports used for their preparation. This fact indicates that the impregnation of hydrated zirconia with trifluoromethanesulfonic acid did not appreciably affect the crystalline characteristics.

On the other hand, the FT-IR spectra of the zirconia gel after being leached with distilled water did not present any of the characteristic bands of urea, as that assigned to the C=O group at 1660 cm^{-1} [16], showing that the template removal by water extraction was effective.

The FT-IR spectrum of the Zr$_{T100}$ sample (Fig. 6) displayed an intense band between 3600 cm^{-1} and 3200 cm^{-1} and another one at 1600 cm^{-1}, assigned to the stretching vibrations of hydroxo- and aquo-OH, and to the bending vibration of (H–O–H) and (O–H–O) present in the structure of the solid, respectively [17–19]. Also, in the energy interval below 850 cm^{-1}, the wide band due to Zr–O stretching vibration is observed.

FT-IR spectra of Zr$_{T200}$, Zr$_{T300}$, and Zr$_{T400}$ supports showed features similar to those observed for the Zr$_{T100}$ sample, though the intensity of the bands at 1600 cm^{-1} and 3600 cm^{-1} decreased when the calcination temperature increased, in parallel with the reduction of the S_{BET}.

The FT-IR spectrum of the TriZr$_{T100}$ sample displayed bands at 1267 cm^{-1}, 1180 cm^{-1}, and 1040 cm^{-1}, in addition to those present in the Zr$_{T100}$ sample (Fig. 6). The first two bands are ascribed to the S=O stretching mode and the last one is assigned to the C–F stretching mode [16], thus showing the presence of trifluoromethanesulfonic acid adsorbed on the support. These bands are also present in the spectra of TriZr$_{T200}$, TriZr$_{T300}$, and TriZr$_{T400}$ catalysts, although with lower intensity as a result of the lower amount of triflic acid adsorbed on the support.

The acidity measurements of the catalysts by means of potentiometric titration with n-butylamine let us estimate the number of acid sites and their acid strength. It was suggested that the initial electrode potential (E_i) indicates the maximum acid strength of the sites, and the value of meq amine/g solid where the plateau is reached indicates the total number of acid sites. The acid strength of these sites may be classified according to the following scale: $E_i > 100$ mV (very strong sites), $0 < E_i < 100$ mV (strong sites), $-100 < E_i < 0$ (weak sites) and $E_i < -100$ mV (very weak sites) [20].

The potentiometric titration results indicated that the TriZr$_{T100}$, TriZr$_{T200}$, TriZr$_{T300}$, and TriZr$_{T400}$ catalysts present very strong acid sites, with E_i potential values between 650 mV and 700 mV, and that the potential decreased more quickly when the temperature of the thermal treatment increased (Fig. 7a), indicating a total number of acid site decrease at higher temperatures. Values of 4.5, 3.5, 3 and 2 meq amine/g solid for TriZr$_{T100}$, TriZr$_{T200}$, TriZr$_{T300}$, and TriZr$_{T400}$, respectively, were obtained. On the other hand, the potentiometric titration curves of the supports were very similar to each other, with E_i being around 360 mV (Fig. 7b).

So, the acid strength of the catalysts is nearly independent of N$_{Tri}$, and much higher than that of the supports. In addition, the number of acid sites decreased in an almost linear relation with the N$_{Tri}$ decrease. As was previously stated, N$_{Tri}$ was dependent on the hydroxylation degree of the support resulting from the thermal treatment applied, which not only affected the S_{BET} of the materials but also, and particularly, the number of sites in which the triflic acid can firmly interact.

The esterification reaction is a type of organic reaction of considerable industrial interest, and it is generally carried out in liquid phase. The mechanism of this reaction homogeneously catalyzed by acids is well known [21], and involves the protonation of the carboxylic oxygen, giving a delocalized carbocation, which can be nucleophilically attacked by an alcohol. The loss of a proton of the adduct produces the intermediary. The protonation of each hydroxylic oxygen leads to water elimination to give the ester. The addition of alcohol excess or water extraction from the reaction medium favors the esterification by displacing the equilibrium.

The mechanism of the reaction carried out employing heterogeneous catalysis can follow an Eley–Rideal (ER) of unique site or a Langmuir–Hinshelwood (LH) of dual site mechanism [22,23], which depends on the type of material employed as catalyst and the working conditions. For exchange resins, it was suggested that the esterification in liquid phase occurs between the protonated adsorbed alcohol and the acid in the liquid phase [24,25] or by a dual site mechanism [26]. In turn, for zeolites, mesoporous solids, zirconia modified with different additives, such as tungstated zirconia, it was reported that the reaction proceeds by a unique site

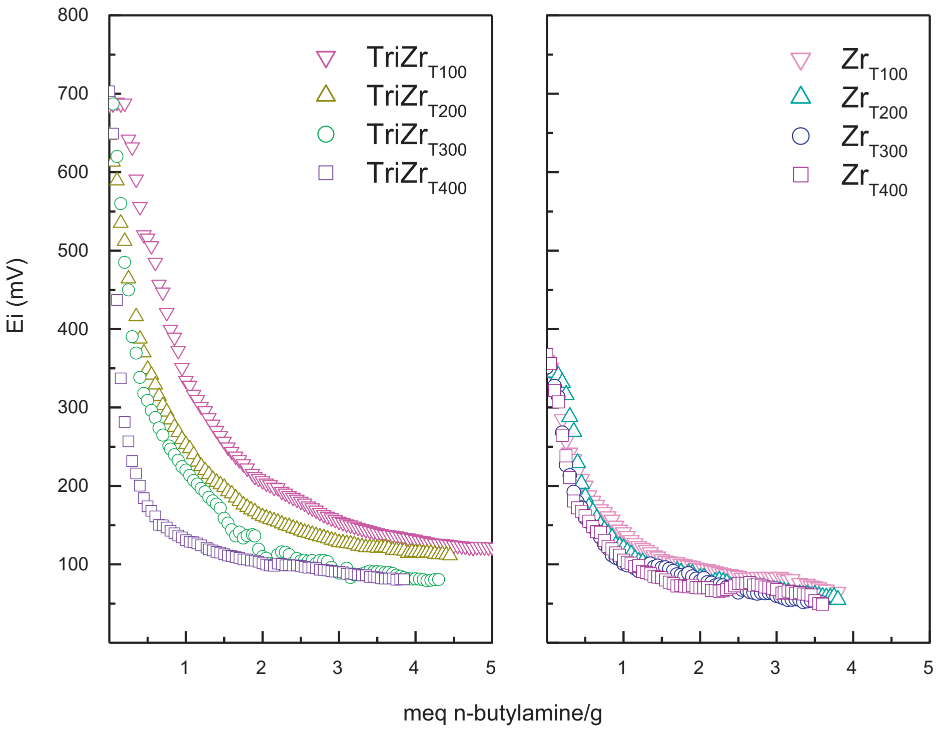

Fig. 7. Potentiometric titration curves of the TriZr$_{T100}$, TriZr$_{T200}$, TriZr$_{T300}$, and TriZr$_{T400}$ samples (a), and those of the respective supports (b).

mechanism, with the acid adsorbed on the catalytic site, followed by reaction with the alcohol from the liquid phase [23,27,28].

The prepared catalysts were tested in the esterification of p-hydroxybenzoic acid with n-propyl alcohol (Scheme 2). The synthesis of propyl paraben was carried out in a conventional batch glass reactor at atmospheric pressure and 100 °C, with a high alcohol:acid molar ratio to favor the displacement of the reaction and a catalyst amount optimized from exploratory results.

It was observed that the amount of p-hydroxybenzoic acid converted into the ester continuously increased with the reaction time (Fig. 8). Furthermore, after 5 h, the reached conversion depended strongly on the CF_3SO_3H content, decreasing from 80% to 7% (Table 3) when N_{Tri} decreased from 0.91 mmol to 0.10 mmol CF_3SO_3H/g. On the other hand, the experiences performed using the supports as catalyst showed a negligible conversion (<2%).

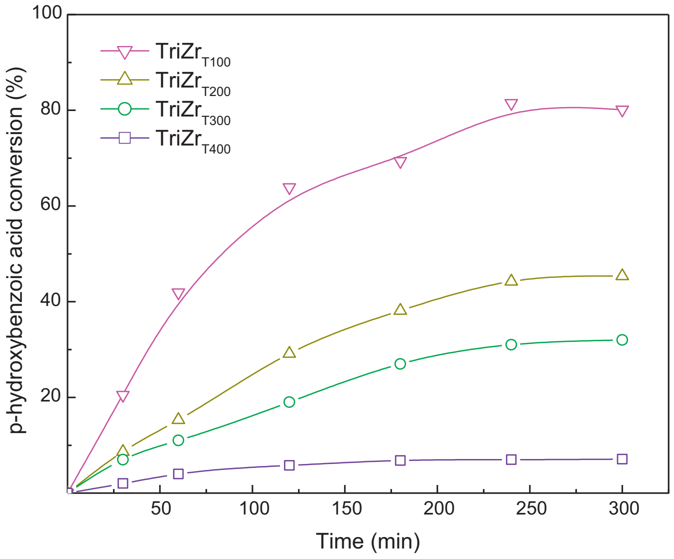

Fig. 8. Conversion of p-hydroxybenzoic acid in propyl paraben synthesis using the TriZr$_{T100}$, TriZr$_{T200}$, TriZr$_{T300}$, and TriZr$_{T400}$ samples as catalysts.

Under the working conditions, it was found that the catalysts are selective, and only traces of propyl ether were detected by means of MS-GC.

The specific catalytic activity (SCA) of the samples, expressed as moles of ester formed at 5 h/mol CF_3SO_3H in the catalyst, decreased slightly in the following order TriZr$_{T100}$ > TriZr$_{T200}$ > TriZr$_{T300}$ > TriZr$_{T400}$ (Table 3), an ordering similar to that followed by the number of acid sites present in the catalysts. A similar conclusion was reported by Landge et al. [29] for toluene benzoylation using Zr-TMS functionalized with triflic acid as catalyst.

After separating the catalyst TriZr$_{T100}$ from the reaction medium, it was washed with ethanol and dried, and then it was reused several times with a slight loss of catalytic activity. While the amount of p-hydroxybenzoic acid converted into propyl paraben with the fresh catalyst was 80%, a value of 77% was obtained in the first reuse and 75% in the second reuse. The TriZr$_{T100}$ catalyst after the second reuse displayed S_{BET}, N_{Tri} and E_i values similar to those of the fresh one.

On the other hand, the tests performed with the purpose of comparing the catalytic behavior of the TriZr$_{T100}$ catalyst in the synthesis of the propyl, ethyl and methyl esters of p-hydroxybenzoic acid were carried out in an autoclave reactor, because it was not

Table 3
Catalytic behavior of the catalysts in propyl paraben synthesis.

Sample	p-hydroxybenzoic acid conversion (%)	SCA[a] (mol ester/mol CF_3SO_3H)
TriZr$_{T100}$	80	8.8
TriZr$_{T200}$	45	8.6
TriZr$_{T300}$	32	7.6
TriZr$_{T400}$	7	7.1

[a] SCA: specific catalytic activity at 5 h.

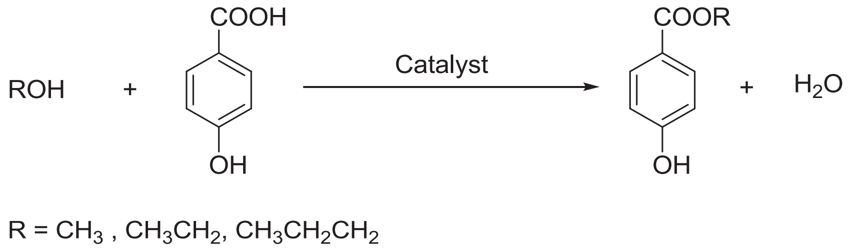

Scheme 2.

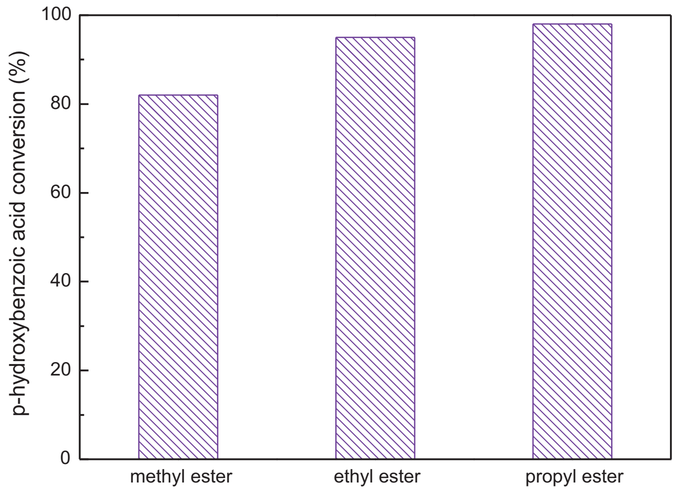

Fig. 9. p-hydroxybenzoic acid conversion in the synthesis of methyl, ethyl and propyl parabens.

possible to obtain the ethyl and methyl parabens in the previous conditions. The results obtained at 5 h under reaction were 98% conversion for the obtainment of propyl paraben, 95% for ethyl paraben, and 82% for methyl paraben (Fig. 9).

As can be observed, under the employed conditions, in which the same ratio was used for the three alcohols, the conversion decreases for the alcohols with shorter chain.

According to Climent et al. [30], a conversion increase with the increment of the alcohol chain length in this type of reaction is due to a higher alcohol hydrophobicity, thus allowing a better alcohol interaction with the carbonylic carbon of the carbocation formed by the carboxylic acid adsorption on the catalyst. It must also be taken into account that the conversion decrease observed in obtaining the parabens corresponding to alcohols with shorter chain can be the result of the lower boiling point of the alcohols, which showed the following ordering: n-propyl alcohol (97 °C) > ethyl alcohol (78.4 °C) > methyl alcohol (64.7 °C).

In brief, the desired products were selectively obtained with very good yields using trifluoromethanesulfonic acid adsorbed on zirconia as catalyst.

4. Conclusions

The parabens were prepared using trifluoromethanesulfonic acid immobilized on zirconia. The oxide was obtained by the sol–gel method, using urea as a pore-forming agent, and it was a mainly mesoporous solid. When the calcination temperature of the support was increased, the specific surface area and the microporous contribution to this area decreased, and at the same time the mean pore diameter increased. The impregnation of the supports with triflic acid, and the subsequent leaching with dichloromethane and diethyl ether led to solid catalysts with CF_3SO_3H tightly adsorbed on the support.

The acid amount depended on the thermal treatment to which the support was subjected. As the increase of the calcination temperature produces the support dehydroxylation, the amount of −OH groups available to firmly adsorb trifluoromethanesulfonic acid decreased, thus decreasing the acid amount.

The prepared catalysts presented very strong acid sites whose number, determined by potentiometric titration, correlated well with the amount of acid firmly attached to the support (N_{Tri}).

Both the acid and textural properties of the catalysts showed that adequate solids to be used as catalysts in acid reactions were obtained. Particularly, the conversion measured in the esterification of p-hydroxybenzoic acid with n-propanol for the synthesis of propyl paraben showed that the conversion definitely depended on the number of acid sites present in the catalysts. This characteristic was, in turn, a result of the preparation conditions of the catalysts, the thermal treatment of the support being the most important parameter, which affected the textural properties and also the amount of trifluoromethanesulfonic acid firmly adsorbed on the support, as a consequence of the dehydroxylation produced when the temperature was increased.

With regard to the esterification reaction to obtain parabens with shorter alkylic chain, slightly lower conversion was obtained under the working conditions used. However, it can be concluded that, in all cases, the prepared materials were selective and led to very good conversion values, thus making them suitable candidates to be used in replacement of classical acids utilized for esterification reactions.

Acknowledgements

The authors thank G. Valle and E. Soto for their experimental contribution, and CONICET and UNLP for the financial support.

References

[1] T. Sabalitschka, in: T.E. Furia (Ed.), CRC Handbook of Food Additives, Vol. 1, CRC Press, Cleveland, Ohio, USA, 1975, pp. 115–184.
[2] M.G. Soni, G.A. Burdock, S.L. Taylor, N.A. Greenberg, Food Chem. Toxicol. 39 (2001) 513–532.
[3] M.G. Soni, S.L. Taylor, N.A. Greenberg, G.A. Burdock, Food Chem. Toxicol. 40 (2002) 1335–1373.
[4] M.G. Soni, I.G. Carabin, G.A. Burdock, Food Chem. Toxicol. 43 (2005) 985–1015.
[5] D.S. Sood, S.C. Sherman, A.V. Iretskii, J.C. Kenvin, D.A. Schiraldi, M.G. White, J. Catal. 199 (2001) 149–153.
[6] R.D. Howells, J.D.Mc. Cown, Chem. Rev. 77 (1977) 69–92.
[7] M. Chamoumi, D. Brunel, F. Fajula, P. Geneste, P. Moreau, J. Solofo, Zeolites 14 (1994) 282–289.
[8] M. Chidambaram, C. Venkatesan, P.R. Rajamohanan, A.P. Singh, Appl. Catal. A: Gen. 244 (2003) 27–37.
[9] D.O. Bennardi, G.P. Romanelli, J.C. Autino, L.R. Pizzio, Catal. Commun. 10 (2009) 576–581.
[10] D.O. Bennardi, G.P. Romanelli, J.C. Autino, L.R. Pizzio, Appl. Catal. A: Gen. 324 (2007) 62–68.
[11] B.-Y. Zhao, X.-P. Xu, H.-R. Ma, D.-H. Sun, J.-M. Gao, Catal. Lett. 45 (1997) 237–244.
[12] J.C. Duchet, M.J. Tilliette, D. Cornet, Catal. Today 10 (1991) 507–520.
[13] T. Yamaguchi, Catal. Today 20 (1994) 199–218.
[14] S. Ajaikumar, A. Pandurangan, J. Mol. Catal. A: Chem. 266 (2007) 1–10.
[15] L.R. Pizzio, Mater. Lett. 60 (2006) 3931.
[16] L.J. Bellamy, The Infrared Spectra of Complex Molecules, Wiley, New York, 1960.

[17] S. Patel, N. Purohit, A. Patel, J. Mol. Catal. A: Chem. 192 (2003) 195–202.
[18] J. Rubio, J.L. Otero, M. Villegas, P. Duran, J. Mater. Sci. 32 (1997) 643.
[19] J.A.R. Van Veen, F.T.G. Veltmaat, G. Jonkers, J. Chem. Soc., Chem. Commun. (1985) 1656.
[20] V.M. Fuchs, L.R. Pizzio, M.N. Blanco, Eur. Polym. J. 44 (2008) 801–807.
[21] I. Roberts, H.C. Urey, J. Am. Chem. Soc. 60 (1938) 2391.
[22] L.R. Pizzio, M.N. Blanco, Appl. Catal. A: Gen. 255 (2003) 265–277.
[23] D.E. López, K. Suwannakarn, J.G. Goodwin Jr., D.A. Bruce, Ind. Eng. Chem. Res. 47 (2008) 2221–2230.
[24] M. Altiokka, A. Citak, Appl. Catal. A: Gen. 239 (2003) 141–148.
[25] C.S.M. Pereira, S.P. Pinho, V.M.T.M. Silva, A.E. Rodríguez, Ind. Eng. Chem. Res. 47 (2008) 1453–1463.
[26] H.T.R. Teo, B. Saha, J. Catal. 228 (2004) 174–182.
[27] Y. Liu, E. Lotero, J.G. Goodwin Jr., J. Catal. 242 (2006) 278–286.
[28] S.R. Kirumakki, N. Nagaraju, K.V.R. Chary, Appl. Catal. A: Gen. 299 (2006) 185.
[29] S.M. Landge, M. Chidambaram, A.P. Singh, J. Mol. Catal. A: Chem. 213 (2004) 257–266.
[30] M.J. Climent, A. Corma, S. Iborra, S. Miquel, J. Primo, F. Rey, J. Catal. 183 (1999) 76.